NANO LETTERS

Letter

pubs.acs.org/NanoLett

Wastewater Mediated Activation of Micromotors for Efficient Water Cleaning

Sarvesh Kumar Srivastava,* Maria Guix, and Oliver G. Schmidt

Institute for Integrative Nanosciences, IFW Dresden, Helmholtzstraße 20, 01069 Dresden, Germany

Supporting Information

ABSTRACT: We present wastewater-mediated activation of catalytic micromotors for the degradation of nitroaromatic pollutants in water. These next-generation hybrid micromotors are fabricated by growing catalytically active Pd particles over thin-metal films (Ti/Fe/Cr), which are then rolled-up into self-propelled tubular microjets. Coupling of catalytically active Pd particles inside the micromotor surface in the presence of a 4-nitrophenol pollutant (with $NaBH_4$ as reductant) results in autonomous motion via the bubble−recoil propulsion mechanism such that the target pollutant mixture (wastewater) is consumed as a fuel, thereby generating nontoxic byproducts. This study also offers several distinct advantages over its predecessors including no pH/temperature manipulation, limited stringent process control and complete destruction of the target pollutant mixture. The improved intermixing ability of the micromotors caused faster degradation ca. 10 times higher as compared to its nonmotile counterpart. The high catalytic efficiency obtained via a wet-lab approach has promising potential in creating hybrid micromotors comprising of multicatalytic systems assembled into one entity for sustainable environmental remediation and theranostics.

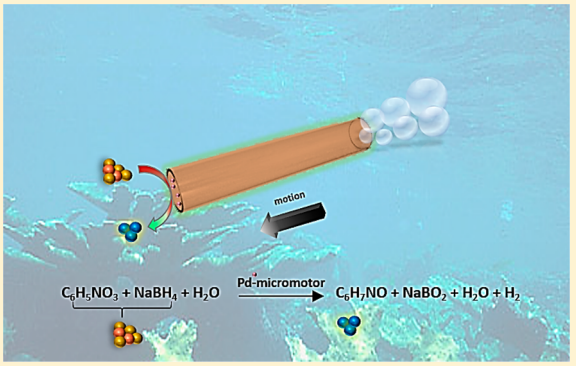

KEYWORDS: *Hybrid micromotors, bubble propulsion, pollutant activated, heterogeneous catalyst, green chemistry*

Water contamination due to increasing anthropogenic activity and limited sustainable cleanup strategies affects millions of people around the world. Aquatic pollution with nitroaromatic compounds poses a major environmental threat owing to its recalcitrant nonbiodegradable nature and extensive usage in the industrial production of dyes, pesticides, and explosives among others.[1] 4-Nitrophenol (4-NP) is one such organic pollutant, which is widely used in synthesis of drugs, fungicides, and leather processing and is leached out as an industrial waste requiring immediate attention.[2−4] Therefore, there is an urgent need to remove such toxic compounds with efficient and noninvasive catalytic systems. At this point, it is important to note that most of the above-mentioned industrial and commercial processes like leather processing, textile/pulp industries, and photographic film production also utilize huge quantities of sodium borohydride ($NaBH_4$) along with 4-NP as required. For example, in tanneries, $NaBH_4$ has been used for aging of leather,[5] while 4-NP is also utilized for preservation and darkening of leather. Similarly, 4-NP is an essential parameter for photographic film development, while $NaBH_4$ is employed to recover silver (precious metal) after its treatment.[6]

Therefore, we see that several industrial processes generate effluent wastewater consisting of 4-NP and $NaBH_4$, requiring further treatment before their discharge. For the same reason, several interesting concepts have been reported for catalytic degradation of 4-NP pollutant (with $NaBH_4$ as reductant) by using metal polyelectrolyte brushes,[7] metal−polymer dendrimers,[8] TiO_2 mediated photocatalytic degradation,[9] bimetallic composites,[10] as well as biogenic materials.[11,12] It is important to note that, in all the above-described catalytic methods for 4-NP pollutant degradation, the wastewater study consists of 4-NP along with $NaBH_4$ to initiate the catalytic degradation reaction via a formation of nitrophenolate ion complex as extensively discussed later in this manuscript.

Today's micro and nanomotors inhere huge potential for both biomedical[13] and environmental applications where motion can be induced by different energy sources including light, magnetic, and electric fields, ultrasonic waves, or chemical fuels.[14] Among them, chemically powered micromotors governed by the bubble−recoil mechanism,[15,16] (among others)[17] have been extensively studied, both for their motion mechanisms[18−20] and improved mixing effects observed during their motion.[21−23] These catalytic micromotors can be regarded as asymmetric, confined geometries of heterogeneous catalysts, promoting high turnover numbers under the aqueous reaction environment. With advances in nanosciences,[24] micromotors have been reported for environmental applications including capture and isolation of certain contaminants as well as water monitoring and remediation.[25−32] However, we see that, although several interesting features have been reported

Received: December 9, 2015
Revised: December 15, 2015

DOI: 10.1021/acs.nanolett.5b05032
Nano Lett. XXXX, XXX, XXX−XXX

Scheme 1. (A) Illustrating Mandatory Conditions for 4-NP Reduction Process with Inset Image Showing 4-Nitrophenolate Ion Solution (Yellow) Acting As Our Pollutant Mixture and (B) Reaction Mechanism of 4-NP Reduction in the Presence of Reductant ($NaBH_4$) on the Surface of Pd-Catalyst

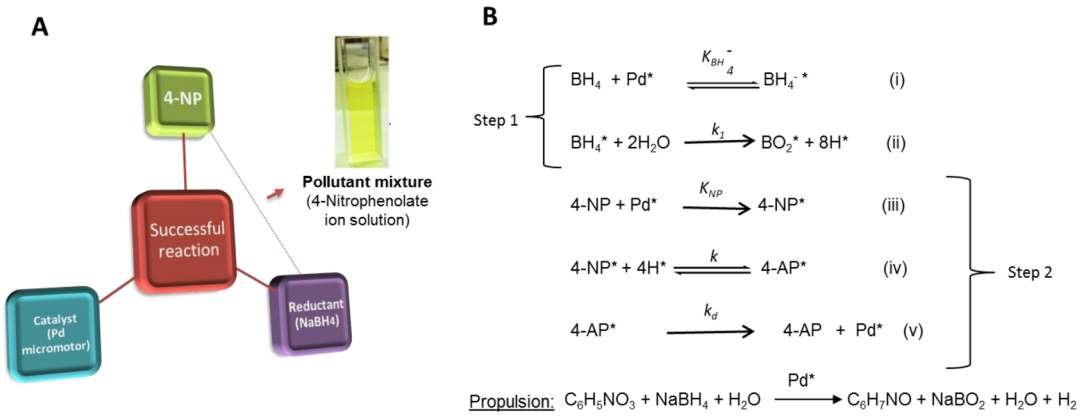

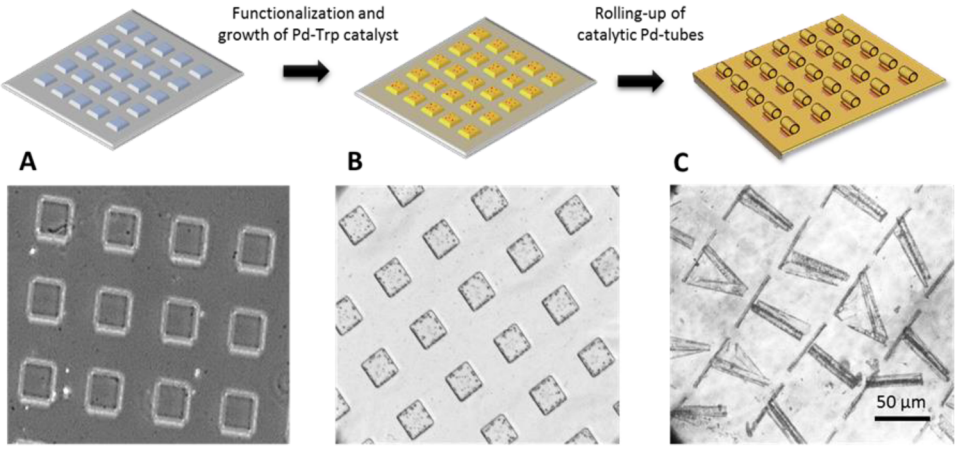

Figure 1. Sequential representation of the fabrication of Pd catalyst grown rolled-up tubes.

above and elsewhere for the development of micromotors, most of these studies still require external fuel solely for propulsion, thereby greatly limiting their application. Also, most of the micromotor studies require addition of surfactants (absent in our case); photocatalytic micromotors cannot function efficiently under the water surface (high energy inputs) where such persistent organic pollutants actually accumulates; UV-mediated photoactivation instantly kills any microbiota which is essential for sustainable remediation over a period of time; or carbon/mesoporous material incorporated nondestructive adsorption of the pollutant which requires additional cleanup. As of now, it is rather imperative that these micromotors tend to behave more efficiently than their heterogeneous catalyst counterpart owing to their micromixing effects via a gas evolution reaction. Therefore, there is an urgent need to innovate newer systems which minimize the use of external fuels, surfactants, and unsustainable energy/environmental processes.

In this study, we chose 4-NP owing to its "model candidate" status (see Scheme 1A) where the degradation proceeds via a catalytic reaction involving three compulsory reaction components namely 4-NP, reductant ($NaBH_4$) and the catalyst (Pd micromotors) along with the formation of a relatively nontoxic product 4-aminophenol (4-AP).[33] This can also be well understood by the study done by Pozun et al. clearly showing that the 4-NP reduction reaction takes place at the metal particle surface and not in the solution, even at the higher concentrations of the reducing agent ($NaBH_4$).[10] This is also in accordance with the study done by Esumi et al.[8] where the use of metal particles (acting as heterogeneous catalyst) showed that $NaBH_4$ transfers surface hydrogen to the available site of the catalyst. Thereafter, 4-NP is adsorbed onto the surface as well where they react to form the reaction product. This wastewater comprising of 4-NP and $NaBH_4$ mixture is a mandatory requirement for catalytic degradation of 4-NP (see Scheme 1A) even under in situ remediation practices and serves as the fuel for our catalytic Pd-micromotor. The associated degradation study can be easily monitored by a spectrophotometer due to the fact that 4-NP aqueous solution is colorless but shows intense yellow color upon addition of $NaBH_4$ due to the formation of 4-nitrophenolate ion, red-shifting the absorption peak to 400 nm.[33,34] The degradation reaction does not proceed in absence of the catalyst, and the absorbance peak with characteristic yellow color tends to remain for several days (as highlighted in the inset image A) of Scheme 1).[35] It must be noted that, although there are studies utilizing external fuel sources for micromotor propulsion (like peroxides,[36] hydrazine,[37] and metal borohydride[38]), the rationale of this research is based on the fact that $NaBH_4$ is a compulsory reaction component for 4-NP degradation (acting as the reductant) and *must not* be confused with addition of an external fuel solely for propulsion. The catalytic reduction of 4-

DOI: 10.1021/acs.nanolett.5b05032
Nano Lett. XXXX, XXX, XXX−XXX

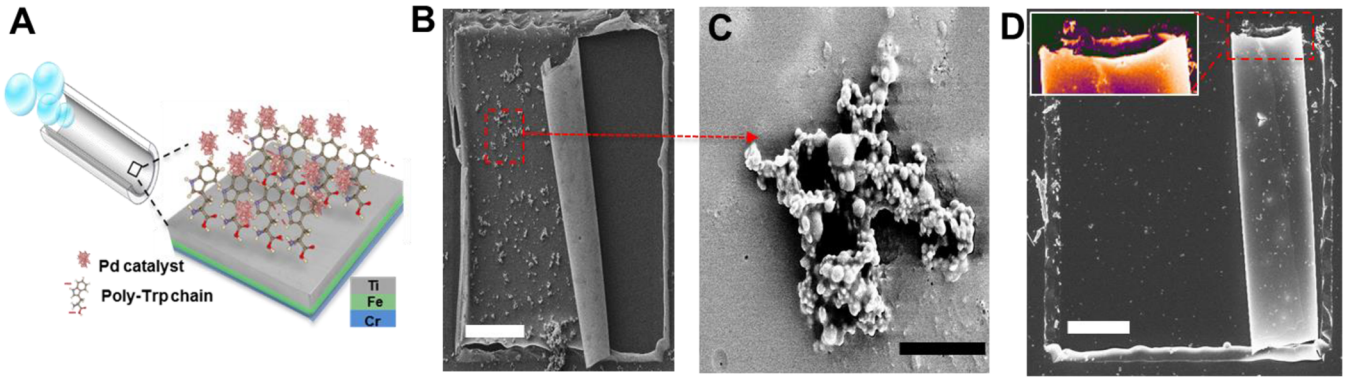

Figure 2. (A) Schematic representation of Pd particles growth over the thin-film unrolled substrate. SEM images showing (B) rolling-up of microtubes with inset (red) highlighting Pd particle assembly. (C) Characteristic dendrite shaped micronetwork assembly of Pd particles. (D) Fully rolled-up microtube with inset image highlighting well-packed loading of catalytic dendrimers. Scale bars: A = 25 μm, B, D = 10 μm, C = 2 μm.

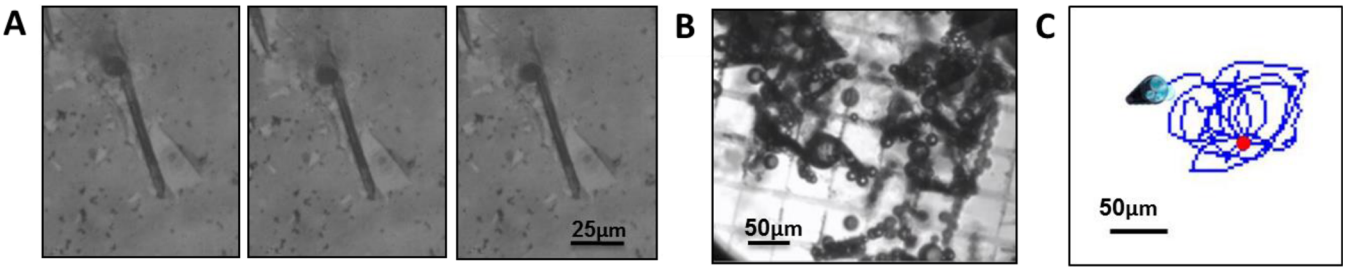

Figure 3. (A) Optical images of bubble formation inside rolled-up structures previously loaded with Pd catalysts at (L to R) 0, 0.185, and 0.233 s, respectively. (B) Homogeneous activation of Pd-loaded micromotors in the presence of 0.001 mM 4-AP and 0.03 mM $NaBH_4$, the pollutant of interest.

NP by Pd particles in the presence of $NaBH_4$ can be explained as shown in Scheme 1B.[39] This can be understood by an in-depth review by Zhao et al.[33] concluding that "both reactants (4-NP and $NaBH_4$) adsorb on the surface of the particles before the reaction. The adsorption of both substrates is fast, and it is modeled in terms of an equilibrium process described by a Langmuir isotherm. The adsorbed species then react, and finally the reaction product dissociates from the surface" as explained in Scheme 1B. It should be noted that, while 4-NP rapidly degrades to the relatively low-toxic product 4-AP (commonly used in drug formulations, hair dyes etc.),[40] $NaBH_4$ also forms a nontoxic borate/metaborate which is essentially a part of the soil, as well as food/water additive,[41] highlighting the green chemistry behind our work.[42]

We fabricated pollutant mixture-activated micromotors by growing Pd-catalytic particles over the unrolled thin-film metallic substrate and rolled them up into catalytic microtubes, as depicted in Figure 1.

Figure 1A represents the first stage of grid functionalization by thermal decomposition of tetrahydrofuran (THF) to allow subsequent Pd particle growth over the surface. Next, a Pd-Trp mixture for catalyst formation was introduced by drop casting over the THF-functionalized substrate resulting in rapid reduction of Pd(II) and forming dendrimer shaped Pd particles (as later discussed with SEM) stabilized via a polymer-like Trp interface (poly-Trp) (Figure 1b). Finally, the active grid was cleaned and rolled-up into catalytically active microtubes of 50 μm in length and ~8 μm in diameter (Figure 1c).

Scanning electron microscopy (SEM) was carried out to examine the surface morphology of catalytic Pd particles grown over the microtube surface (see Figure 3).

We observed a highly uneven surface with multiple dendrimer shaped Pd clusters packed together resulting in a distinct micro network (0.1 to ~2 μm) growing on the inner side of the rolled-up tube, as highlighted in Figure 2A and B.[43] Figure 2C shows highly uneven Pd particles (highlighted region of Figure 2B) with a characteristic "crest and trough" landscape which is responsible for a high catalytic activity due to large surface area and efficient binding with the active sites. Figure 2D shows the optimal loading of Pd catalyst once grown and rolled-up inside the 50 μm long and 8 μm wide micromotor. It should be noted that the resulting Pd-surface morphology is highly desirable as much of the catalytic efficiency needed for hydrogen evolution via hydrolysis of $NaBH_4$ present in the reaction mixture is attributed to the surface roughness and support matrix of the catalyst.[44−47] This was further confirmed when we observed that no propulsion effect was observed by e-beam deposited Pd layer (10 nm) over thin films (see Video S3 in SI). We were able to achieve the same by incorporating a rough surface morphology with a stable organic support for our catalytic microtubes as confirmed by XPS (see Figure S1 in Supporting Information)

Figure 3A reveals that the motion principle behind our catalytic micromotors is based on the bubble-recoil mechanism (see Video S4 in SI). This is evident in Figure 3A highlighting the three stages of initial nucleation, growth, and release of the bubble inside the tubular structure.[16] Figure 3B shows homogeneous activation of Pd grown rolled-up micromotors with distinct bubble formation once they are introduced in the reaction environment (see Video S5 in SI). These micromotors were able to attain an appreciable speed of about 270 μm/s in the presence of the pollutant mixture as inferred from the tracking data highlighted in Figure 3C (see Video S7 in SI).

DOI: 10.1021/acs.nanolett.5b05032
Nano Lett. XXXX, XXX, XXX−XXX

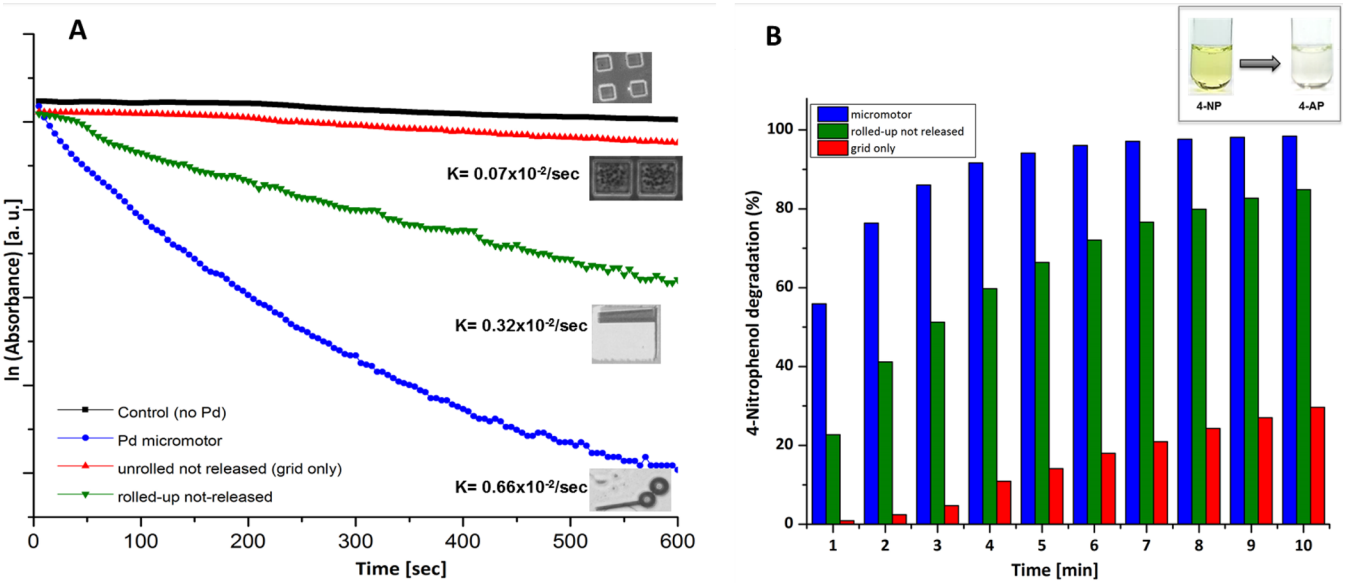

Figure 4. (A) 4-NP degradation as a function of absorbance (400 nm) vs time (sec) and associated reaction constant. (B) Percentage degradation of 4-NP over the course of reaction (10 min). Inset showing 4-NP pollutant mixture (yellow) being degraded in 4-AP (colorless) over the course of reaction.

We compared the catalytic efficiency of motile micromotors with that of immotile rolled-up tubes fixed to the surface, and the silicon grid containing only flat unrolled metallic thin films as support. Figure 4A shows the decrease in $\ln(A)$ with respect to time and the associated reaction constant (k) for all three reaction mixtures. A piece of silicon grid (Ti:Fe:Cr) with surface functionalization but no Pd catalyst was also used as a control (black line). We observed that the Pd-micromotors offered fastest degradation activity as observed in terms of reaction constant (k) to be 0.66×10^{-2}/sec highlighted in Figure 4A. The reaction constant in case of "rolled up but not released" and "grid only" was found to be $k = 0.32 \times 10^{-2}$/s and $k = 0.07 \times 10^{-2}$/s, respectively. This indicates that our tubular microjets have superior catalytic performance due to better distribution or availability of reactants across the active site of Pd catalyst.

This is in agreement with a previously reported study where self-propelled micromotors performed better due to the fluid convection and vortex streams were created along with the micromotor's movement.[22,23] In the present study, the rate of degradation in case of grid alone (without rolling up or releasing) by the virtue of Pd catalytic particles was less as compared to its inclusion inside the rolled-up tubes (4.5 times) and highest in case of micromotors (9.5 times) which were released in the reaction mixture. Owing to its extremely efficient reaction kinetics (Figure 4B), Pd-micromotors were able to degrade over 55% of 4-NP within the first minute of the reaction as compared to only 22% and 1% for the "rolled-up and not released" and "grid alone" case, respectively. Within the half-time of the reaction (5 min), micromotors were able to degrade over 95% of 4-NP and went on to achieve 99% degradation by the end of the reaction period (10 min). This is crucial as the degradation percentage of "rolled-up not released" and "grid only" was found to be 85% and 30% respectively. The associated color change in all of these reaction mixtures was also visually distinguished at the end of the reaction (see Video S6 in SI).

In conclusion, we have shown pollutant mixture activated micromotors for rapid degradation of organic pollutants in water. Most importantly, unlike any previously reported studies, there was no addition of external fuels solely to achieve propulsion (like hydrogen peroxide), pH manipulation, or temperature change, thereby marking a significant step forward in mimicking the real in situ detoxification conditions. Upon completing their degradation activity, these micromotors can be easily recovered using a magnet with no remaining toxic byproducts. The high catalytic efficiency obtained by the growth of a catalyst open new avenues to create hybrid micromotors with multipollutant specificity owing to different catalytic systems assembled onto them for efficient waste management. Owing to its extremely efficient performance and distinct advantages over its counterparts, the next-generation of pollutant-activated hybrid micromotors can have broad implications for sustainable environmental remediation, multi-analyte sensing and enabling multistep reactions for advanced "microengine enabled propulsion". Finally, we have opened a new dimension for chemical engineers to fabricate efficient catalytic systems to find exciting applications in the ever growing field of motile micromotors/mechanics.

■ ASSOCIATED CONTENT

Supporting Information

The Supporting Information is available free of charge on the ACS Publications website at DOI: 10.1021/acs.nanolett.5b05032.

Additional details about methods and analytical results (XPS) (PDF)

Comparative evaluation of the rolling efficiency of the Ti/Fe/Cr thin films by isoproanol and aq acetone (MPG)

Rolling-up and releasing of Pd-grown catalytic micromotors via aq acetone mixture (MPG)

Rolled-up e-beam deposited Pd (10 nm) microtubes in the presence of 4-NP reaction mixture (MPG)

DOI: 10.1021/acs.nanolett.5b05032
Nano Lett. XXXX, XXX, XXX−XXX

Bubble nucleation and release in Pd-catalytic microtubes in the presence of 4-NP reaction mixture (1000 fps) (MPG)
Homogeneous activation of Pd-grown micromotors in the presence of 4-NP pollutant mixture (MPG)
Real time visualization (color change from yellow to colorless) of 4-NP degradation by grid only, rolled-up not released and rolled-up released (micromotor) (16×) (MPG)
Single micromotor motion (normal and diluted 4× pollutant mixture) (MPG)

AUTHOR INFORMATION

Corresponding Author

*E-mail: sarvesh.kumar@ifw-dresden.de.

Notes

The authors declare no competing financial interest.

ACKNOWLEDGMENTS

SKS would like to thank Deutscher Akademischer Austauschdienst (DAAD)-Leibniz for funding. The authors thank Yan Chen for help with SEM and Dr. Steffen Oswald for XPS analysis.

REFERENCES

(1) Kovacic, P.; Somanathan, R. *J. Appl. Toxicol.* **2014**, *34*, 810−824.
(2) ATSDR. *ATSDR Toxicological Profile for Nitrophenols: 2-Nitrophenol and 4-Nitrophenol*; ATSDR: Atlanta, 2005.
(3) Yen, J.-H.; Lin, K.-H.; Wang, Y.-S. *Ecotoxicol. Environ. Saf.* **2002**, *52*, 113−116.
(4) Fonger, G. C. *Toxicology* **1995**, *103*, 137−145.
(5) Covington, A. D.; Covington, T. *Tanning Chemistry: The Science of Leather*; Royal Society of Chemistry, 2009.
(6) Wang, L. K.; Hung, Y. T.; Lo, H. H.; Yapijakis, C. *Handbook of Industrial and Hazardous Wastes Treatment*; CRC Press, 2004.
(7) Mei, Y.; Lu, Y.; Polzer, F.; Ballauff, M.; Drechsler, M. *Chem. Mater.* **2007**, *19* (5), 1062−1069.
(8) Hayakawa, K.; Yoshimura, T.; Esumi, K. *Langmuir* **2003**, *19*, 5517−5521.
(9) Lee, H.-G.; Sai-Anand, G.; Komathi, S.; Gopalan, A.-I.; Kang, S.-W.; Lee, K.-P. *J. Hazard. Mater.* **2015**, *283* (0), 400−409.
(10) Pozun, Z. D.; Rodenbusch, S. E.; Keller, E.; Tran, K.; Tang, W.; Stevenson, K. J.; Henkelman, G. *J. Phys. Chem. C* **2013**, *117* (15), 7598−7604.
(11) Srivastava, S. K.; Yamada, R.; Ogino, C.; Kondo, A. *Nanoscale Res. Lett.* **2013**, *8*, 70.
(12) Srivastava, S.; Ogino, C.; Kondo, A. In *Green Processes for Nanotechnology SE - 8*; Basiuk, V. A., Basiuk, E. V, Eds.; Springer International Publishing, 2015; pp 237−257.
(13) Srivastava, S. K.; Medina-Sánchez, M.; Koch, B.; Schmidt, O. G. *Adv. Mater.* **2015**, 4327.
(14) Guix, M.; Mayorga-Martinez, C. C.; Merkoçi, A. *Chem. Rev.* **2014**, *114* (12), 6285−6322.
(15) Mei, Y.; Huang, G.; Solovev, A. A.; Ureña, E. B.; Mönch, I.; Ding, F.; Reindl, T.; Fu, R. K. Y.; Chu, P. K.; Schmidt, O. G. *Adv. Mater.* **2008**, *20*, 4085−4090.
(16) Solovev, A. A.; Mei, Y.; Ureña, E. B.; Huang, G.; Schmidt, O. G. *Small* **2009**, *5*, 1688−1692.
(17) Yamamoto, D.; Mukai, A.; Okita, N.; Yoshikawa, K.; Shioi, A. *J. Chem. Phys.* **2013**, *139*, 034705.
(18) Fomin, V. M.; Hippler, M.; Magdanz, V.; Soler, L.; Sanchez, S.; Schmidt, O. G. *IEEE Trans. Robot.* **2014**, *30*, 40−48.
(19) Li, L.; Wang, J.; Li, T.; Song, W.; Zhang, G. *Soft Matter* **2014**, *10* (38), 7511−7518.
(20) Li, J.; Huang, G.; Ye, M.; Li, M.; Liu, R.; Mei, Y. *Nanoscale* **2011**, *3*, 5083.
(21) Campuzano, S.; Kagan, D.; Orozco, J.; Wang, J. *Analyst* **2011**, *136*, 4621.
(22) Soler, L.; Magdanz, V.; Fomin, V. M.; Sanchez, S.; Schmidt, O. G. *ACS Nano* **2013**, *7*, 9611−9620.
(23) Morales-Narváez, E.; Guix, M.; Medina-Sánchez, M.; Mayorga-Martinez, C. C.; Merkoçi, A. *Small* **2014**, *10*, 2542−2548.
(24) Khin, M. M.; Nair, A. S.; Babu, V. J.; Murugan, R.; Ramakrishna, S. *Energy Environ. Sci.* **2012**, *5*, 8075.
(25) Garcia-Gradilla, V.; Orozco, J.; Sattayasamitsathit, S.; Soto, F.; Kuralay, F.; Pourazary, A.; Katzenberg, A.; Gao, W.; Shen, Y.; Wang, J. *ACS Nano* **2013**, *7*, 9232−9240.
(26) Guix, M.; Orozco, J.; Garcia, M.; Gao, W.; Sattayasamitsathit, S.; Merkoči, A.; Escarpa, A.; Wang, J. *ACS Nano* **2012**, *6*, 4445−4451.
(27) Gao, W.; Pei, A.; Wang, J. *ACS Nano* **2012**, *6*, 8432−8438.
(28) Jurado-Sánchez, B.; Sattayasamitsathit, S.; Gao, W.; Santos, L.; Fedorak, Y.; Singh, V. V.; Orozco, J.; Galarnyk, M.; Wang, J. *Small* **2015**, *11* (4), 499−506.
(29) Li, J.; Singh, V. V.; Sattayasamitsathit, S.; Orozco, J.; Kaufmann, K.; Dong, R.; Gao, W.; Jurado-Sanchez, B.; Fedorak, Y.; Wang, J. *ACS Nano* **2014**, *8* (11), 11118−11125.
(30) Singh, V. V.; Martin, A.; Kaufmann, K.; de Oliveira, S. D. S.; Wang, J. *Chem. Mater.* **2015**, *27* (23), 8162−8169.
(31) Wani, O. M.; Safdar, M.; Kinnunen, N.; Jänis, J. *Chem. - Eur. J.* **2015**, n/a.
(32) Mushtaq, F.; Guerrero, M.; Sakar, M. S.; Hoop, M.; Lindo, A. M.; Sort, J.; Chen, X.; Nelson, B. J.; Pellicer, E.; Pane, S. *J. Mater. Chem. A* **2015**, *3* (47), 23670−23676.
(33) Zhao, P.; Feng, X.; Huang, D.; Yang, G.; Astruc, D. *Coord. Chem. Rev.* **2015**, *287* (0), 114−136.
(34) Panigrahi, S.; Basu, S.; Praharaj, S.; Pande, S.; Jana, S.; Pal, A.; Ghosh, S. K.; Pal, T. *J. Phys. Chem. C* **2007**, *111*, 4596−4605.
(35) Ghosh, S. K.; Mandal, M.; Kundu, S.; Nath, S.; Pal, T. *Langmuir* **2004**, *268*, 61−66.
(36) Paxton, W. F.; Kistler, K. C.; Olmeda, C. C.; Sen, A.; St Angelo, S. K.; Cao, Y.; Mallouk, T. E.; Lammert, P. E.; Crespi, V. H. *J. Am. Chem. Soc.* **2004**, *126* (41), 13424−13431.
(37) Gao, W.; Pei, A.; Dong, R.; Wang, J. *J. Am. Chem. Soc.* **2014**, *136* (6), 2276−2279.
(38) Singh, V. V.; Soto, F.; Kaufmann, K.; Wang, J. *Angew. Chem., Int. Ed.* **2015**, *54* (23), 6896−6899.
(39) Bingwa, N.; Meijboom, R. *J. Phys. Chem. C* **2014**, *118* (34), 19849−19858.
(40) Komatsu, T.; Hirose, T. *Appl. Catal., A* **2004**, *276*, 95−102.
(41) Şahin, Ö.; Genli, N.; Özdemir, M. *Chem. Eng. Process.* **2005**, *44*, 1−6.
(42) European Commission. *Scientific Committee on Consumer Products Opinion on para-Aminophenol COLIPA no. A16*; 2005, p 40, http://ec.europa.eu/health/ph_risk/committees/04_sccp/docs/sccp_o_00e.pdf (accessed Dec 17, 2015).
(43) Kannan, P.; Dolinska, J.; Maiyalagan, T.; Opallo, M. *Nanoscale* **2014**, *6* (19), 11169−11176.
(44) Patel, N.; Patton, B.; Zanchetta, C.; Fernandes, R.; Guella, G.; Kale, A.; Miotello, A. *Int. J. Hydrogen Energy* **2008**, *33*, 287−292.
(45) Karmakar, P.; Ghose, D. *Nucl. Instrum. Methods Phys. Res., Sect. B* **2004**, *222*, 477−483.
(46) Abe, H.; Uchida, H.; Azuma, Y.; Uedono, A.; Chen, Z. Q.; Itoh, H. *Nucl. Instrum. Methods Phys. Res., Sect. B* **2003**, *206*, 224−227.
(47) Zhang, Z.; Xiao, F.; Xi, J.; Sun, T.; Xiao, S.; Wang, H.; Wang, S.; Liu, Y. *Sci. Rep.* **2014**, *4*, 4053.

DOI: 10.1021/acs.nanolett.5b05032
Nano Lett. XXXX, XXX, XXX−XXX